

Simultaneous Path Following and Obstacle Avoidance Control of a Unicycle-type Robot

Lionel Lapierre, Rene Zapata and Pascal Lepinay

Abstract—This paper proposes an algorithm that drives a unicycle type robot to a desired path, including obstacle avoidance capabilities. The path following control design relies on Lyapunov theory, backstepping technics and deals explicitly with vehicle dynamics. Furthermore, it overcomes initial condition constraint present in a number of path following control strategies described in the literature. This is done by controlling explicitly the rate of progression of a "virtual target" to be tracked along the path; thus bypassing the problems that arise when the position of the path target point is simply defined as the closest point on the path. The obstacle avoidance part is using the Deformable Virtual Zone principle, that defines a safety zone around the vehicle, in which the presence of an obstacle induces an "intrusion of information" that drives the vehicle reaction. The overall algorithm is combined with a guidance solution that embeds the path following requirements in a desired intrusion information function, that steers the vehicle to the desired path while the DVZ is virtually keeping a minimal contact with the obstacle, implicitly bypassing it. Simulation and experimental results illustrate the performance of the control system proposed.

I. INTRODUCTION

Real-time obstacle avoidance coupled with an accurate path following control is one of the major issue in the field of mobile robotics [10], [3]. The underlying problems to be solved can be divided in three issues:

- path following control of non-holonomic systems,
- obstacle avoidance strategy,
- the coupling between the two previous goals.

The general underlying assumption in path following control is that the vehicle's forward velocity tracks a desired speed profile, while the controller acts on the vehicle orientation to drive it to the path. See the works of Micaeli *et al* [8], Samson *et al* [12] for pioneering work in the area as well as Canudas de Wit *et al* [4], Jiang *et al* [7] and Soetanto *et al* [13] and the references therein. The main contributions of the method exposed in [13] are :

- i) it extends the results obtained by Micaeli *et al* in [8] - for kinematic wheeled robots - to a more general setting, in order to deal with vehicle dynamics and parameter uncertainty,
- ii) it overcomes stringent initial condition constraint that are present in a number of path following control strategies in the literature. This is done by controlling explicitly the rate of progression of a *virtual target* to be tracked along the path, thus bypassing the problems that arise when the position of the target point on the path is simply defined by the projection of the actual vehicle on the path. This

procedure avoids the singularities that occur when the vehicle is located at the current center of curvature of the path virtual target location (where the closest point is not unique), and allows for global convergence of the vehicle to the desired path. This is in contrast with the results described by Micaeli *et al* in [8] for example, where only local convergence is proven.

Obstacle avoidance strategy is another major issue to perform reliable applications in the field of mobile robotics, and underlies two different issues:

- the obstacle detection,
- the computation of the system reaction.

The obstacle detection is an important topic but is not the subject of this paper. Then, the system is assumed to be equipped with sensor devices able to estimate the distance between the robot and the surrounding environment.

The system reaction can be considered at the high level (Path replanning) or directly in the controller as a *reflex behavior*. The reaction quantification is generally made according to an arbitrary positive potential field functions attached on obstacles that repels the robot, and an attractive field located on the goal. The main difficulty of this method is to design an artificial potential function without undesired local minima. Elnagar *et al*, in [5], propose to model the potential field by Maxwell's equations that completely eliminate the local minima problem, with the condition that an *a priori* knowledge of the environment is available. These methods are generally computationally intensive. Iniguez *et al*, in [6], proposes a hierarchical and dynamic method, that works on a non regular grid decomposition, simple and computationally efficient, both in time and memory. Another approach, based on a *reflex behavior* reaction, is using the *Deformable Virtual Zone* (DVZ) concept, in which a robot kinematic dependent *risk zone* is located on the robot, surrounding it. The deformation of this zone is due to the intrusion of proximity information. The system reaction is made in order to reform the *risk zone* to its nominal shape, implicitly repelling the obstacles. For a clear exposition of the DVZ principle, please refer to [14].

In this paper we propose to investigate the coupling between the path following algorithm described in [13] with a DVZ based reactive obstacle avoidance control. The proposed method consists in a guidance solution that embeds the path following requirements in a desired proximity function (with respect to the obstacles) that drives the robot to contour the obstacles while guaranteeing the path following convergence requirements when there is no obstacle. This approach is based on the derivation of a Lyapunov function that

The three authors are with the Laboratory for Computer Science, Microelectronics and Robotics, 161 Rue Ada, 34392 Montpellier Cedex 5, France (lapierre, zapata, lepinay)@lirmm.fr

guarantees the asymptotic convergence to the path without obstacles, and the boundedness of a variable called *intrusion ratio*, that captures the surrounding obstacles proximity and the current robot situation with respect to the path. The combination of path following with a reactive - local - obstacle avoidance strategy has a natural limitation coming from the situation where both controllers yield antagonist system reactions. In this proposed method, this situation leads to a local minimum called the *corner situation*, where a heuristic switch between controllers is necessary. The advantage of the method is that outside this very specific *corner situation*, no switch is required.

The paper is organized as follows: section 2 and 3 review the basic algorithms we will use for path following and obstacle avoidance. Section 4 shows our solution to combine both the controllers and section 5 illustrates the results we have obtained. Finally section 6 presents the conclusion and further work of this study.

II. BASIC ALGORITHMS: PATH FOLLOWING AND OBSTACLE AVOIDANCE

A. Path following control

This section briefly reviews a solution for the problem of steering a unicycle type vehicle along a desired path.

Classic assumptions are made regarding the robot (see figure 1 and [13] for details). The wheels control provides the forward force F and angular torque N applied on the vehicle's center of mass.

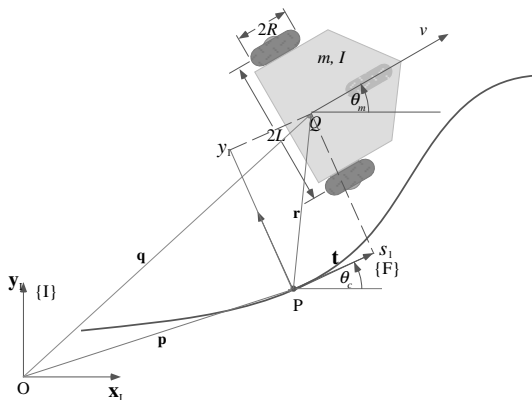


Fig. 1. Path Following: frames definition and problem pose description.

1) *Kinematic equations of motion. The Serret - Frenet Frame:* Motivated by the work developed by A. Micaelli and C. Samson in [8] a Frenet frame $\{F\}$ that moves along the path to be followed is used. The significant difference with this work of is: *the Frenet frame is not attached to the point on the path that is closest to the vehicle.* Instead, the origin of $\{F\}$ along the path evolves according to a conveniently defined function of time, effectively yielding an extra controller design parameter. This seemingly simple procedure allows to lift the stringent initial condition constraints that arise with the path following controlled described in [8].

Consider Figure 1, where P is an arbitrary point on the path to be followed and Q is the center of mass of the moving vehicle. Associated with P , consider the corresponding Serret-Frenet frame $\{F\}$. The signed curvilinear abscissa of P along the path is denoted s . Clearly, Q can either be expressed as $\mathbf{q} = (X, Y)$ in a selected inertial reference frame $\{I\}$ or as (s_1, y_1) in $\{F\}$. Stated equivalently, Q can be given in (X, Y) or (s_1, y_1) coordinates. Let \mathbf{R} be the rotation matrix from $\{I\}$ to $\{F\}$, parameterized locally by the angle θ_c . Define $\omega_c = \dot{\theta}_c$. Then,

$$\begin{cases} \omega_c = \dot{\theta}_c = c_c(s)\dot{s} \\ \dot{c}_c(s) = g_c(s)\dot{s} \end{cases} \quad (1)$$

where $c_c(s)$ and $g_c(s) = \frac{dc_c(s)}{ds}$ denote the path curvature and its derivative, respectively.

The velocity of the unicycle in the $\{I\}$ frame satisfies the equation

$$\begin{bmatrix} \dot{X} \\ \dot{Y} \end{bmatrix} = u \begin{bmatrix} \cos \theta_m \\ \sin \theta_m \end{bmatrix} \quad (2)$$

where θ_m and u denote the yaw angle of the vehicle and its body-axis speed, respectively. The introduction of the variable $\theta = \theta_m - \theta_c$ gives the kinematic model of the unicycle in the (s_1, y_1) coordinates as

$$\begin{cases} \dot{s}_1 = -\dot{s}(1 - c_c y_1) + u \cos \theta \\ \dot{y}_1 = -c_c \dot{s} s_1 + u \sin \theta \\ \omega = \dot{\theta} = \omega_m - c_c \dot{s} \end{cases} \quad (3)$$

where $\omega_m = \dot{\theta}_m$.

2) *Dynamics. Problem Formulation:* The dynamical model of the unicycle is obtained by augmenting (3) with the equations

$$\begin{cases} \dot{u} = \frac{F}{M} \\ \dot{\omega} = \frac{N}{\mathcal{I}} - c_c \dot{s} - g_c \dot{s}^2 \end{cases} \quad (4)$$

where $\dot{\omega}_m = \frac{N}{\mathcal{I}}$ and M and \mathcal{I} are the mass and the moment of inertia of the unicycle, respectively. Let F_{PF} and N_{PF} the path following control inputs.

With the above notation, the problem under study can be formulated as follows:

Given a desired speed profile $u_d(t) > u_{min} > 0$ for the vehicle speed u , derive a feedback control law for F_{PF} and N_{PF} to drive y_1 , θ , and $u - u_d$ asymptotically to zero.

3) Nonlinear Controller Design:

This section introduces a nonlinear closed loop control law to steer the dynamic model of a wheeled robot described by (3)-(4) along a desired path. Controller design builds on previous work by Micaelli *et al* [8] on path following control and relies heavily on backstepping technics.

We now state the proposed solution of the problem exposed in section 2.

Proposition 1: *consider the kinematic and dynamic models described in (3) and (4). Let the approach angle $\delta(y_1, u)$ be*

$$\delta(y_1, u) = -\mathbf{sign}(u)\theta_a \frac{e^{2k_\delta y_1} - 1}{e^{2k_\delta y_1} + 1} \quad (5)$$

where $0 < \theta_a < \pi/2$ and k_δ an arbitrary positive gain. Assume that $u_d(t)$ is a C^2 function and that $\lim_{t \rightarrow \infty} u_d(t)$

is different from zero. Suppose the path to be followed is parameterized by its curvilinear abscissa s and assume that for each s the variables θ , s_1 , y_1 , c_c and g_c are well defined. The dynamic control law

$$\begin{aligned} N_{PF} &= \mathcal{I} \left(\ddot{\delta} - k_1(\dot{\theta} - \dot{\delta}) - k_2(\theta - \delta) + c_c \dot{s} + g_c \dot{s} \right) \\ F_{PF} &= \mathcal{M} (\dot{u}_d - k_3(u - u_d)) \\ \dot{s} &= u \cos \theta + k_s s_1 \end{aligned} \quad (6)$$

where k_1 , k_2 , k_3 and k_s are arbitrary positive gains, drives y_1 , s_1 and θ asymptotically to zero.

Indication of proof. The key steps in the proof can be briefly described as follows: let $V_1 = \frac{1}{2} [(\theta - \delta)^2 + (u - u_d)^2 + (r - r_d)^2]$ be a Lyapunov candidate, where $r_d = \dot{\delta} - k_1(\theta - \delta)$. The control (6) yields $\dot{V}_1 \leq 0$. Since \dot{V}_1 is negative semi definite and bounded below, V_1 is bounded and has a limit. Therefore, s_1 , y_1 , θ and u are bounded since δ and u_d are assumed to be bounded. From the equation above, it then follows that \dot{s}_1 , \dot{y}_1 , $\dot{\theta}$ and \dot{u} are bounded as well. It is now easy to compute the second derivative of V_1 and prove it is bounded. Therefore, \dot{V}_1 is uniformly continuous and Barbalat's lemma implies that $\dot{V}_1 \rightarrow 0$ as $t \rightarrow \infty$, that induces the asymptotic convergence of s_1 , y_1 , θ and u . Then the vehicle is asymptotically driven to the path.

Remark. The computation of the second derivative of V_1 requires the derivation of the approach angle expression δ , that is discontinuous around $u = 0$. A rigorous proof should consider an approach angle expression as, for instance $\delta = -\theta_A \tanh k_\delta y_1 u$ that is differentiable everywhere. The use of this previous expression makes the control derivation more complex, bringing new considerations on the convergence rate when u is small. For the sake of simplicity, we are ignoring this discontinuity around $u = 0$ and consider that \dot{V}_1 is bounded everywhere.

B. Obstacle avoidance algorithm

This section presents an obstacle avoidance algorithm based on the use of a continuous *Deformable Virtual Zone* (DVZ). The main idea is to define the robot/environment interaction as a DVZ surrounding the vehicle (cf. figure 2). The deformation of this *risk zone* Ξ is due to the intrusion of proximity information and thus control the robot reactions. This DVZ characterizes the deformable zone geometry, and depends on the robot velocities (forward and rotational velocities, u and r). Briefly, the risk zone, disturbed by obstacle intrusion, can be reformed by acting on the robot velocities.

1) *The undeformed DVZ:* In order to acquire an analytical expression of the polar signature of the undeformed DVZ, expressed in the robot frame $\{B\}$, we consider an elliptical shape, see figure 3. Straightforward computation yields:

$$d_h(\alpha) = \frac{-B + \sqrt{B^2 - 4AC}}{2A} \quad (7)$$

where

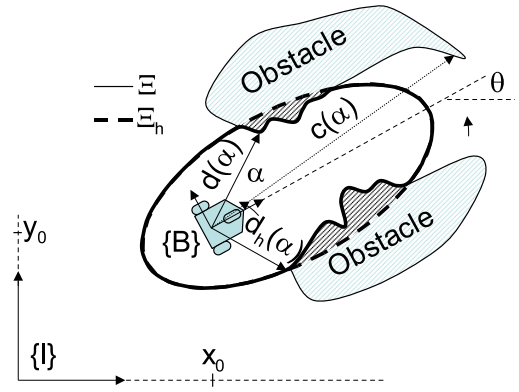


Fig. 2. Obstacle Avoidance: frames definition and problem pose description.

$$\begin{aligned} A &= (c_y \cos(\alpha - \gamma))^2 + (c_x \sin(\alpha - \gamma))^2 \\ B &= 2 \cdot (a_x \cos(\alpha - \gamma)c_y^2 + a_y \sin(\alpha - \gamma)c_x^2) \\ C &= (a_x c_y)^2 + (a_y c_x)^2 - c_x^2 c_y^2 \end{aligned} \quad (8)$$

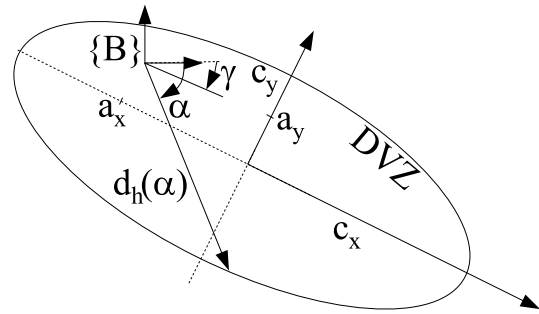


Fig. 3. The undeformed DVZ

Moreover, the undeformed DVZ is a function of the robot velocities. We arbitrarily choose the following guidance functions.

$$\begin{aligned} c_x &= \lambda_{c_x} u^2 + c_x^{min} \\ c_y &= \frac{\sqrt{5}}{3} c_x \\ a_x &= -(2/3)c_x \\ a_y &= 0 \end{aligned} \quad (9)$$

Considering that the DVZ is rigidly attached to the robot, oriented in the main direction of the vehicle movement, we state $\gamma = 0$.

2) *The deformed DVZ:* The deformed DVZ is acquired from the sensor information, denoted $c(\alpha)$. Since the meaningful information is restricted to the one inside the undeformed DVZ, a preliminary test on the sensor information is necessary.

$$\begin{aligned} d(\alpha) &= c(\alpha) \text{ if } c(\alpha) < d_h, \\ &= d_h(\alpha) \text{ elsewhere} \end{aligned} \quad (10)$$

3) *The deformation*: The choice of the intrusion information variable expression is instrumental in designing the system reactivity and the closed loop asymptotic system properties. Let

$$I = \int_{\alpha=0}^{2\pi} \frac{d_h(\alpha, u) - d(\alpha)}{d(\alpha)} d\alpha \quad (11)$$

be the intrusion information expression. Note that a null distance robot/obstacle yields an infinite intrusion information. Thus a control that warrants a bounded intrusion information at any time, induces the system to avoid any obstacle.

4) *System Jacobian functions*: The time derivation of the expression of the intrusion information yields

$$\dot{I} = J_I^u \dot{u} + J_I^\theta r + F^{Rob.vel} u + F^{Obst.vel} \quad (12)$$

with

$$\begin{aligned} J_I^u &= \int_{\alpha=0}^{2\pi} \frac{1}{d(\alpha)} \left(\frac{1}{2A} \left[-J_B^u + \frac{B J_B^u - 2C J_A^u - 2A J_C^u}{\sqrt{B^2 - 4AC}} \right] \right) d\alpha \\ J_I^\theta &= \int_{\alpha=0}^{2\pi} \frac{-1}{d(\alpha)} \left(\frac{1}{2A} \left[-J_B^\gamma + \frac{B J_B^\gamma - 2C J_A^\gamma}{\sqrt{B^2 - 4AC}} \right] \right) d\alpha \\ F^{Rob.vel} &= \int_{\alpha=0}^{2\pi} \frac{d_h(\alpha)}{d^2(\alpha)} \cos \alpha d\alpha \\ F^{Obst.vel} &= \int_{\alpha=0}^{2\pi} \frac{d_h(\alpha)}{d^2(\alpha)} \begin{pmatrix} -[\dot{x}_E \cos(\theta_m + \alpha) \\ + \dot{y}_E \sin(\theta_m + \alpha)] \end{pmatrix} d\alpha \end{aligned} \quad (13)$$

where

$$\begin{aligned} J_A^u &= 2(c_y \frac{\partial c_y}{\partial u} \cos^2(\alpha) + c_x \frac{\partial c_x}{\partial u} \sin^2(\alpha)) \\ J_A^\gamma &= 2 \cos(\alpha) \sin(\alpha) (c_y^2 - c_x^2) \end{aligned} \quad (14)$$

$$J_B^u = 2 \begin{pmatrix} \cos(\alpha) [c_y^2 \frac{\partial a_x}{\partial u} + 2a_x c_y \frac{\partial c_y}{\partial u}] \\ + \sin(\alpha) [c_x^2 \frac{\partial a_y}{\partial u} + 2a_y c_x \frac{\partial c_x}{\partial u}] \end{pmatrix} \quad (15)$$

$$J_B^\gamma = 2 (a_x c_y^2 \sin(\alpha) - a_y c_x^2 \cos(\alpha))$$

$$J_C^u = 2 \begin{pmatrix} a_x c_y [c_y \frac{\partial a_x}{\partial u} + a_x \frac{\partial c_y}{\partial u}] \\ + a_y c_x [c_x \frac{\partial a_y}{\partial u} + a_y \frac{\partial c_x}{\partial u}] \\ - c_x c_y [c_x \frac{\partial c_y}{\partial u} + c_y \frac{\partial c_x}{\partial u}] \end{pmatrix} \quad (16)$$

and \dot{x}_E, \dot{y}_E define the obstacle absolute velocity. The assumption of static obstacles yields $F^{Rob.vel} = 0$. For the sake of simplicity, we consider now only static obstacles.

5) *Obstacle Avoidance Control Design*: Let the following Lyapunov candidate $V_I = \frac{I^2}{2}$. The derivation yields

$$\dot{V}_I = I(J_I^u \dot{u} + J_I^\theta r + F^{Rob.vel} u) \quad (17)$$

It is straightforward to see that the choice

$$\begin{cases} \dot{u} = -K_u J_I^u I - \frac{F^{Rob.vel}}{J_I^u} u \\ r = -K_r J_I^\theta I \end{cases} \quad (18)$$

where K_u, K_r are arbitrary positive gains yields $\dot{V}_I \leq 0 \forall t$. Note that tedious but straightforward computation (using for the sake of simplicity the guidance functions in (9)) shows

that the term $\frac{F^{Rob.vel}}{J_I^u}$ is a positive function that acts as a non linear damping term. That confirms the well posedness of the expression (18).

The control (18) is an hybrid kinematic/dynamic solution. A Backstepping step is necessary for the torque control. Let $V_{OA} = \frac{1}{2}(r_d - r)^2$ be a Lyapunov candidate, where $r_d = -K_r J_I^\theta I$. The choice $\dot{r} = \dot{r}_d - K_r(r - r_d)$ yields $\dot{V}_{OA} \leq 0$. Then the dynamic obstacle avoidance control is written as

$$\begin{cases} F_{OA} = \mathcal{M} \left(-K_u J_I^u I - \frac{F^{Rob.vel}}{J_I^u} u \right) \\ N_{OA} = \mathcal{I} (\dot{r}_d - K_r(r - r_d)) \end{cases} \quad (19)$$

where K_r and K_u are arbitrary positive gains, \mathcal{M} and \mathcal{I} are the mass and moment of inertia of the vehicle, and $r_d = -K_r J_I^\theta I$.

III. COMBINING PATH FOLLOWING AND OBSTACLE AVOIDANCE

A. Mathematical inspiration

The combination of the two algorithms is solved as a guidance problem. The requirements are:

- the vehicle should remain far from the obstacle, i.e. in presence of obstacle I has to be bounded at any time,
- when there is no obstacle, the vehicle has to asymptotically converge to the desired path.

To do so, we rewrite the obstacle avoidance control, adding a desired intrusion information $I_d = K_d \tanh(\lambda_d(\theta - \delta))$, where K_d and λ_d are arbitrary positive gains, θ and δ are path following variables defined in the previous chapter (equations(3) and (5)). Let $V_2 = \frac{(I - I_d)^2}{2}$ be a Lyapunov candidate. It is straightforward to see that the choice

$$\begin{cases} r = -K_r(I - I_d)(J_I^\theta - I'_d) + c_c \dot{s} + \dot{\delta} \\ \dot{u} = -K_u J_I^u (I - I_d) - \frac{F^{Rob.vel}}{J_I^u} u \end{cases} \quad (20)$$

implies that $I - I_d$ asymptotically converges to a bounded set defined as:

$$|I - I_d|_{t \rightarrow \infty} < \frac{J_I^\theta (c_c \dot{s} + \dot{\delta})}{K_r (J_I^\theta - I'_d)^2 + K_u (J_I^u)^2} \quad (21)$$

where $I'_d = \frac{2K_d \lambda_d}{1 + (\lambda_d(\theta - \delta)^2)}$. Note that the previous expression is bounded since $(J_I^u)^2 > 0$ if $u \neq 0$, I'_d is bounded and if the quantity $c_c \dot{s} + \dot{\delta}$ is assumed to be bounded. This last requirement is covered by the assumption that the free space is connected.

Then, contouring the obstacle, the vehicle cannot be driven infinitely far from the desired path, i.e. $c_c \dot{s} + \dot{\delta}$ remains bounded. Moreover, if there is no obstacle, the Lyapunov candidate degenerates in $V_{I=0} = \frac{I_d^2}{2}$, and the previous control choice yields $\dot{V}_{I=0} = -K_r I_d^2 I'_d \leq 0$, that induces the path following asymptotic convergence requirements. The dynamic control corresponding to the previous solution is

$$\begin{cases} F_{OA} = \mathcal{M} \left(-K_u J_I^u (I - I_d) - \frac{F^{Rob.vel}}{J_I^u} u \right) \\ N_{OA} = \mathcal{I} (r_d - K_r(r - r_d)) \end{cases} \quad (22)$$

where $r_d = -K_r(I - I_d)(J_I^\theta - I'_d) + c_c \dot{s} + \dot{\delta}$, K_u and K_r are arbitrary positive gains. At this stage one should note

that this solution does not prevent the forward velocity u to be null, and the poor convergence rate around the path. Then we propose another control version that avoids these drawbacks, but by the way loses any mathematical proof of convergence.

B. Practical solution

The combination of path following and obstacle avoidance capabilities has a natural limitation coming from the situation where the both criteria induces antagonist system reactions.

For instance, the obstacle avoidance algorithm may impose the forward velocity to be reduced to zero or a negative value.

This situation occurs when the deformed DVZ Ξ is symmetric with respect to the forward velocity direction. Then the robot will orient itself to minimize the intrusion, and regulates its forward velocity to reshape the nominal DVZ Ξ_h in order to respect the intrusion requirement, i.e. $\lim_{t \rightarrow \infty} I = I_d$. This situation is called *corner situation*, as described in the table IV-A b) and c). To avoid this problematic local minimum, we design the following switching scheme. Let I_l and I_r be the intrusion information on the left ($0 < \alpha < \pi$) and right ($\pi < \alpha < 2\pi$) side, respectively, and $u_{min} > 0$ be the lowest admissible forward velocity. The chosen corner situation detection is made with the following switching condition. The boolean variable *CORNER* is initialized to zero, then

$$\begin{aligned} & \text{if } [(I_l I_r > 0) \& (u < u_{min})] \{CORNER = 1\} \\ & \text{if } (I_l I_r = 0) \{CORNER = 0\} \end{aligned} \quad (23)$$

The reaction to this situation is to

- i) reduce the forward velocity,
- ii) rotate until the obstacle is present only on one side, using the following controllers.

$$\begin{aligned} \dot{u}_{CORNER} &= -K_u u \\ r_{CORNER} &= r_C \text{sign}(I_d) \end{aligned} \quad (24)$$

where K_u is a positive gain, and r_C the chosen rotational velocity to operate the corner extraction. The overall control algorithm is written

$$\begin{aligned} & \text{if } (CORNER = 0) \\ & \{N = N_{OA} + f(I)N_{PF}; F = F_{OA} + f(I)F_{PF}\} \\ & \text{else} \\ & \{N = \mathcal{I}(-K_r(r - r_{CORNER})); F = \mathcal{M}\dot{u}_{CORNER}\} \end{aligned} \quad (25)$$

where the selection function is $f(I) = \frac{1}{1+K_I I}$, with K_I a positive gain. Note that this algorithm imposes the robot to travel with a positive forward velocity $u > u_{min} > 0$, outside the *corner situation*. This warranties the well posedness of the expressions (20), (21) and (22). Then the global control (25) is well posed in any situation.

IV. RESULTS

The previous solution implicitly requires an estimation of \dot{I} in the computation of F_{OA} . The numerical derivation of the sensors information induces a noise amplification and

$K_r^{PF} = 0.1$	$K_u^{PF} = 1$	$K_r^{OA} = 0.01$	$K_u^{OA} = 0.1$
$K_d = 10$	$\lambda_d = 0.01$	$K_I = 100$	$u_d = 1$
$\lambda_{cx} = 100$	$c_x^{min} = 10$	$K_u^{CORNER} = 0.1$	$r_c = 1$

TABLE I

THE CHOSEN CONTROL PARAMETERS

will not provide an accurate estimation of \dot{I} . Therefore, we degrade the previous solution at a kinematic level.

$$\begin{cases} r = r_{OA} + f(I)r_{pf} \\ u = u_{OA} + f(I)u_{pf} \end{cases} \quad (26)$$

where

$$\begin{cases} r_{PF} = \dot{\delta} - K_r^{PF}(\theta - \delta) + c_c \dot{s} \\ u_{PF} = \int_0^t (\dot{u}_d - K_u^{PF}(u - u_d)) dt \\ \dot{s} = u \cos \theta + k_s s_1 \end{cases} \quad (27)$$

$$\begin{cases} r_{OA} = -K_r^{OA}(I - I_d)(J_r - I'_d) + c_c \dot{s} + \dot{\delta} \\ u_{OA} = \int_0^t (-K_u^{OA} J_u (I - I_d) - \frac{F^{rob.vel}}{J_u} u) dt \end{cases}$$

The chosen DVZ guidance functions are chosen according to 9. The other functions are chosen according to the following equations.

$$\begin{aligned} I_d &= K_d \tanh \lambda_d (\theta - \delta) \\ f(I) &= \frac{1}{1+K_I I} \end{aligned} \quad (28)$$

A. Simulation results

We have implemented the algorithm on a unicycle simulator developed with Matlab. The control parameters are chosen according to the table I. The results are displayed in the table 2. The figure 2-a shows the path and obstacles definitions. The robot is of the unicycle type, on which a 32 proximity sensors belt is mounted, displayed as surrounding radial rays of length defined by the nominal DVZ. The figure 2.b indicates a corner situation, on which we see the reduction of the DVZ due to the decreased forward velocity. The next figure 2.c shows the system after the switch from *corner situation* to nominal control. Then the figure 3-d displays the global trajectory the system has made.

B. Experimental results

We have implemented the algorithm on the Peeke robot from the Wany company. This robot is driven with two independent wheels and carries a 16 Infrared proximity sensors belt. The figure 4 displays the odometric trajectory coming from the robot. Since the navigation system is only based on odometric information, the real trajectory does not present significant interest to demonstrate the validity of our approach. The robot clearly avoid obstacle and goes back to the nominal path without requiring switching control. This is valid in this particular situation where the *corner situation* does not occurs. Some chattering behavior has to be filtered out with a gain tuning according to the Peeke ((c)Wany) robot capabilities. The figure 5 shows the evolution of the forward velocity. The black dots are the desired velocity when no obstacle is detected, the stars indicates the evolution of the forward velocity in presence of obstacles.

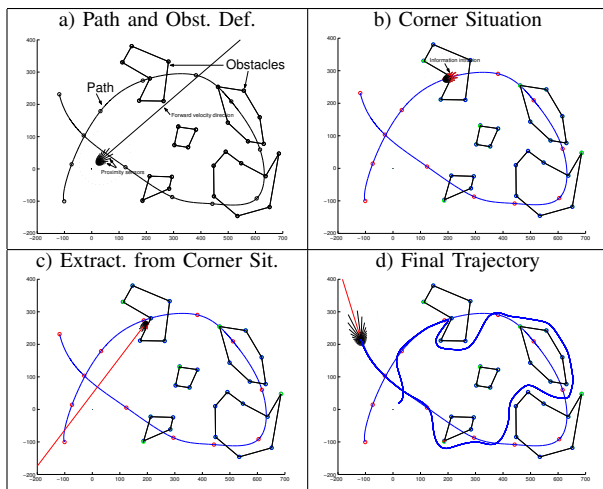


TABLE II
SIMULATION RESULTS

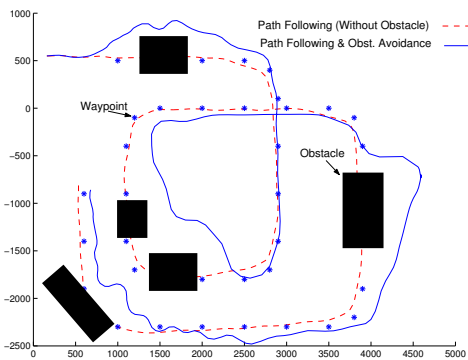


Fig. 4. Experimental results, trajectories

V. CONCLUSION

We have designed a combined path following and obstacle avoidance control law for a unicycle type robot based on the use of the DVZ concept and on the Lyapunov and Backstepping design. The implementation of this solution on the robot Peeke ((c)Wany) illustrates the interesting performances of the solution, in order to avoid some unnecessary *hot switches* when the vehicles travels with an important forward velocity. By this way, we are combining the reactivity of the DVZ principle with a path following control without requiring any path replanning. The next step of this study is to intrinsically attribute the reactivity of the guidance system to the path following virtual target, explicitly controlling the evolution of an added virtual state of the virtual target, along the y_1 direction (see figure (1)). Then the main robot control could be designed as a tracker of a cooperative virtual target; note that the system reactivity is then in charge of a new dynamic guidance system.

VI. ACKNOWLEDGEMENTS

This work is supported by a post doctoral grant from the french national RNTL project WACIF. For

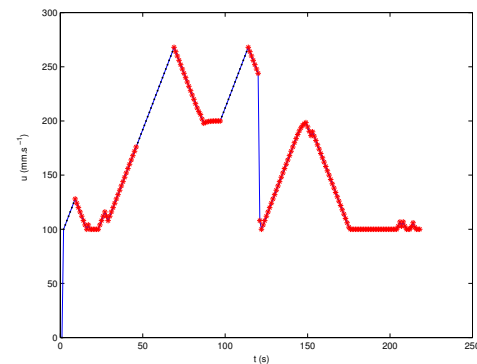


Fig. 5. Experimental results, forward velocity

further information on this project, please contact <http://intranet.wacif.net/default.aspx>.

REFERENCES

- [1] Althaus P. and Christensen H., *Behavior Coordination for Navigation in Office Environment*, IEEE/RSJ International Conference on Intelligent Robots and Systems, Lausanne, Switzerland, October 2002
- [2] Arkin, R.C., *Behavior Based Robotics*, MIT Press, Cambridge, MA., 1998
- [3] Ogren P., *Real-time Obstacle Avoidance for Fast Mobile Robots*, IEEE Trans. on System, Man and Cybernetics, Vol 19, No 5, Sept/Oct 1989, pp. 1179-1187
- [4] Canudas de Wit, C. H. Khennouf, C. Samson and O.J. Sordalen, *Nonlinear Control Design for Mobile Robots*, in Recent Trends in Mobile Robotics (Yuan F. Zheng, Ed.), Vol 11. World Scientific Series in Robotics and Automated Systems. PP. 121-156, 1993
- [5] Elnagar A. and Hussein A., *Motion Planning using Maxwell's equations*, IEEE/RSJ International Conference on Intelligent Robots and Systems, Lausanne, Switzerland, October 2002
- [6] Iniguez P. and Rossel J., *A Hierarchical and Dynamic Method to Compute Harmonic Functions for Constrained Motion Planning*, IEEE/RSJ International Conference on Intelligent Robots and Systems, Lausanne, Switzerland, October 2002
- [7] Z. P. Jiang and H. Nijmeijer, *A recursive Technique for Tracking Control of Nonholonomic Systems in Chained Form*, IEEE Trans. on Robotics and Automation, Vol 44, No 2, 1999, pp. 265-279
- [8] Miccaelli, A. and Samson, C., "Trajectory - Tracking for Unicycle - Type and Two - Steering - Wheels Mobile Robots," *Technical Report No. 2097*, INRIA, Sophia-Antipolis, Nov. 1993
- [9] Ogren P. and Leonard N., *A Provable Convergent Dynamic Window Approach to Obstacle Avoidance*, IFAC World Congress, Barcelona, Spain, July 2002
- [10] Ogren P., *Formation and Obstacle Avoidance in Mobile Robot Control*, Ph.D. Thesis, Stockholm, Norway, June 2003
- [11] Rimón E. and Koditschek D., *Exact Robot Navigation Using Artificial Potential Functions*, IEEE Transactions on Robotics and Automation, pp. 501-518, Vol 8, No. 5, October 1992
- [12] Samson, C. and Ait-Abderrahim, K., "Mobile Robot Control Part 1: Feedback Control of A Non-Holonomic Mobile Robots," *Technical Report No. 1281*, INRIA, Sophia-Antipolis, France, June 1991
- [13] Soetanto, D., Lapiere, L. and Pascoal, A., *Adaptive, Nonsingular path following control of Dynamic wheeled robot*, CDC'03, 42nd IEEE Conference on Decision and Control, Maui, Hawaii, USA, Dec. 2003
- [14] Zapata R., Cacitti A., Lepinay P., *DVZ-based Collision Avoidance Control of Non-holonomic Mobile Manipulators*, JESA, European Journal of Automated Systems, Vol38, Num5, pp. 559-588, 2004.